Higher-Order Vector Finite Elements for Tetrahedral Cells

J. Scott Savage, *Student Member, IEEE*, and Andrew F. Peterson, *Senior Member, IEEE*

Abstract— **Edge-based vector finite elements are widely used for two-dimensional (2-D) and three-dimensional (3-D) electromagnetic modeling. This paper seeks to extend these low-order elements to higher orders to improve the accuracy of numerical solutions. These elements have relaxed normal-component continuity to prohibit spurious modes, and also satisfy Nedelec's constraints to eliminate unnecessary degrees of freedom while remaining entirely local in character. Element matrix derivations are given for the first two vector finite element sets. Also, results of the application of these basis functions to cavity resonators demonstrate the superiority of the higher-order elements.**

I. Introduction

THE FINITE element solution of three-dimensional (3-D) electromagnetic problems using the lowest order vector finite elements, defined by Nedelec on tetrahedra [1], has been well documented [2]–[3]. These elements are commonly referred to as edge elements or Whitney elements. Because the functions do not impose normal-component continuity between cells, they produce no spurious modes in the numerical solution of the curl-curl equation. However, these mixed-order elements, which allow a constant tangential, linear normal (CT/LN) representation of the fields on mesh edges, limit the accuracy of the finite element solution. Higher order basis functions, also proposed by Nedelec, allow for more accurate solutions of 3-D problems, while retaining the benefit of permitting no spurious modes. These functions fall in the general class known as "curl conforming" since they do not impose complete continuity, but do ensure tangential continuity between cells. The next higher order basis functions on tetrahedra provide a linear tangential, quadratic normal (LT/QN) representation of the fields. The basis functions of next higher order have a quadratic tangential, cubic normal (QT/CuN) representation for the fields.

This article reviews these basis functions and provides closed-form expressions for the element matrices arising from the CT/LN and LT/QN functions. In addition, numerical results for the resonant frequencies of 3-D cavities are presented to illustrate the relative accuracy of the higher-order functions and the error trends as the cell sizes are reduced.

II. Basis Function Definition

Table I shows an unnormalized simplex-coordinate representation of CT/LN, LT/QN, and QT/CuN basis functions for a given cell in the finite element mesh. L_i is the simplex coordinate associated with node i of the cell. L_i is unity at node i and decays linearly to zero at the other three nodes of the cell. For edge based functions, i and j represent the two node indices associated with that edge. For face based functions, i, j, and k represent the three node indices at the vertices of that face.

Since CT/LN basis functions have six unknowns associated with any cell, they lead to 6×6 element matrices, while LT/QN and QT/CuN basis functions result in 20×20 and 45×45 element matrices, respectively. Also, CT/LN functions have one unknown per edge throughout the global model, while LT/QN functions have two unknowns per edge and two unknowns per face. QT/CuN functions have three unknowns per edge, six unknowns per face, and three unknowns per tetrahedron. Thus, higher order basis functions lead to more unknowns for a given finite element mesh. Also, higher order basis functions result in global matrices with greater density (more nonzero entries per row and column). Therefore, the computational burden in creating and solving the finite element matrices for a given mesh increases with the order of the basis functions.

The basis function definitions in Table I apply to an individual tetrahedron. Since many tetrahedra may share a certain edge, the global basis functions on that edge straddle each of those tetrahedra. Similarly, up to two tetrahedra may share a common face, so the global basis functions on that face straddle those tetrahedra. This convention ensures tangential field continuity across tetrahedra boundaries throughout the mesh.

III. Element Matrix Derivations

Efficient finite-element analysis of electromagnetic fields in 3-D regions requires computation of two element matrices associated with the curl-curl form of the vector Helmholtz operator [3]. These two matrices are

$$E_{ij} = \int_V \nabla \times \overline{\boldsymbol{B}}_i \cdot \nabla \times \overline{\boldsymbol{B}}_j \, dV \tag{1}$$

and

$$F_{ij} = \int_V \overline{\boldsymbol{B}}_i \cdot \overline{\boldsymbol{B}}_j \, dV \tag{2}$$

where $\overline{\boldsymbol{B}}_i$ represents the ith vector basis function and V indicates integration over one tetrahedron. It is implied that (1) and (2) involve only the portion of each basis function

Manuscript received August 1, 1995; revised February 15, 1996. This work was supported in part by NSF Grant ECS-9257927 and Electromagnetic Sciences, Inc

The authors are with the School of Electrical and Computer Engineering, Georgia Institute of Technology, Atlanta, GA 30332-0250 USA.

Publisher Item Identifier S 0018-9480(96)03802-1.

TABLE I
3-D VECTOR BASIS FUNCTIONS ON TETRAHEDRA

(CT/LN) 6 functions	(LT/QN) 20 functions	(QT/CuN) 45 functions
6 Edge Based	12 Edge Based	18 Edge Based
for all $i<j$, $L_i\nabla L_j - L_j\nabla L_i$	for all $i \neq j$, $L_i\nabla L_j$	for all $i \neq j$, $L_i(2L_i-1)\nabla L_j$, i ≠ j
	8 Face Based	for all $i<j$, $L_iL_j(\nabla L_i - \nabla L_j)$
	for all $i<j<k$, $L_iL_j\nabla L_k - L_iL_k\nabla L_j$ $L_iL_j\nabla L_k - L_jL_k\nabla L_i$	24 Face Based
		for all $i \neq j \neq k$, $L_i(2L_i-1)(L_j\nabla L_k - L_k\nabla L_j)$ $L_i^2(L_j\nabla L_k - L_k\nabla L_j)$
		3 Cell Based
		$L_1L_2L_3\nabla L_4 - L_2L_3L_4\nabla L_1$ $L_1L_2L_4\nabla L_3 - L_2L_3L_4\nabla L_1$ $L_1L_3L_4\nabla L_2 - L_2L_3L_4\nabla L_1$

which lies in a particular cell. A closed-form derivation of these matrices facilitates efficient formation of the global finite element system of equations.

A. CT/LN Elements

This section presents the derivation of element matrices for constant tangent/linear normal CT/LN basis functions. These basis functions are associated with tetrahedra edges and are defined in Table I as

$$\overline{B}_i = l_i(L_{i1}\nabla L_{i2} - L_{i2}\nabla L_{i1}) \qquad i = 1, \cdots, 6. \tag{3}$$

In this representation, L_{i1} is the simplex coordinate associated with the first node of edge i, L_{i2} is the simplex coordinate associated with the second node of edge i, and l_i is the length of edge i. The simplex coordinates for a given cell are

$$L_i = a_i + b_ix + c_iy + d_iz \qquad i = 1, \cdots, 4 \tag{4}$$

and the gradient of any simplex coordinate is

$$\nabla L_i = b_i\hat{x} + c_i\hat{y} + d_i\hat{z}. \tag{5}$$

The simplex coefficients, $a_i \cdots d_i$, can be computed by inverting the coordinate matrix

$$\begin{bmatrix} b_1 & c_1 & d_1 & a_1 \\ b_2 & c_2 & d_2 & a_2 \\ b_3 & c_3 & d_3 & a_3 \\ b_4 & c_4 & d_4 & a_4 \end{bmatrix} = \begin{bmatrix} x_1 & x_2 & x_3 & x_4 \\ y_1 & y_2 & y_3 & y_4 \\ z_1 & z_2 & z_3 & z_4 \\ 1 & 1 & 1 & 1 \end{bmatrix}^{-1} \tag{6}$$

where (x_i, y_i, z_i) is the location of node i. As an intermediate step in computing the inverse of the coordinate matrix, the volume of the tetrahedron, V, is computed. As implied in (6), these simplex coefficients are not normalized to the volume of the tetrahedron.

TABLE II
LOCAL FACE, EDGE, AND NODE CONVENTIONS

Edge #	Node 1	Node 1	
1	1	2	
2	1	3	
3	1	4	
4	2	3	
5	2	4	
6	3	4	
Face #	**Node 1**	**Node 2**	**Node 3**
1	1	2	3
2	1	2	4
3	1	3	4
4	2	3	4

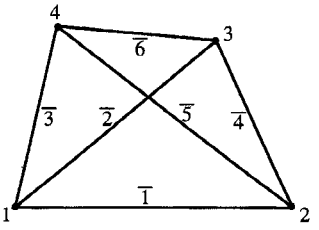

Fig. 1. The node and edge labeling convention used in this document. Face labeling conventions are presented in Table II.

All tetrahedra are given a local structure as illustrated in Fig. 1. The first local node associated with any edge, i_1, is the lesser of the two node numbers adjacent to the edge. Table II presents the convention used for local node, edge, and face numbering. For notational and computational convenience, the following notations are adopted. For two given nodes, i and j, a vector matrix and scalar matrix are defined as

$$\overline{v}_{ij} = \nabla L_i \times \nabla L_j = \hat{x}(c_i d_j - c_j d_i) + \hat{y}(b_j d_i - b_i d_j) + \hat{z}(b_i c_j - b_j c_i) \tag{7}$$

and

$$\phi_{ij} = \nabla L_i \cdot \nabla L_j = b_i b_j + c_i c_j + d_i d_j \tag{8}$$

where each of the simplex coefficients are defined in (6). These matrices are constant for a given cell, and may be obtained as the first step in element matrix computation. Since both $\overline{v}$ and ϕ are independent of position, either may be removed from any integrand. Also, note that $\overline{v}_{ij} = -\overline{v}_{ji}$. The evaluation of the element matrix in (1) requires the curl of each basis function

$$\begin{aligned}\nabla \times \overline{\boldsymbol{B}}_i &= \nabla \times l_i(L_{i1}\nabla L_{i2} - L_{i2}\nabla L_{i1}) \\ &= l_i \nabla \times (L_{i1}\nabla L_{i2}) - l_i \nabla \times (L_{i2}\nabla L_{i1}) \\ &= 2l_i \nabla L_{i1} \times \nabla L_{i2} = 2li\overline{v}_{i1,i2}.\end{aligned} \tag{9}$$

Again, $i1$ and $i2$ are the endpoints of edge i. With this, (1) becomes

$$\begin{aligned}E_{ij} &= 4l_i l_j \int_V \overline{v}_{i1,i2} \cdot \overline{v}_{j1,j2}\, dV \\ &= 4V l_i l_j (\overline{v}_{i1,i2} \cdot \overline{v}_{j1,j2}).\end{aligned} \tag{10}$$

The second element matrix, given in (2), requires the calculation of basis function dot products

$$\begin{aligned}&\overline{\boldsymbol{B}}_i \cdot \overline{\boldsymbol{B}}_j \\ &= l_i(L_{i1}\nabla L_{i2} - L_{i2}\nabla L_{i1}) \cdot l_j(L_{j1}\nabla L_{j2} - L_{j2}\nabla L_{j1}) \\ &= l_i l_j \begin{bmatrix} L_{i1}L_{j1}(\nabla L_{i2} \cdot \nabla L_{j2}) - L_{i1}L_{j2}(\nabla L_{i2} \cdot \nabla L_{j1}) \\ -L_{i2}L_{j1}(\nabla L_{i1} \cdot \nabla L_{j2}) + L_{i2}L_{j2}(\nabla L_{i1} \cdot \nabla L_{j1}) \end{bmatrix}.\end{aligned} \tag{11}$$

Applying the notation of (8), (11) becomes

$$\begin{aligned}\overline{\boldsymbol{B}}_i \cdot \overline{\boldsymbol{B}}_j = l_i l_j [&L_{i1}L_{j1}(\phi_{i2,j2}) - L_{i1}L_{j2}(\phi_{i2,j1}) \\ &- L_{i2}L_{j1}(\phi_{i1,j2}) + L_{i2}L_{j2}(\phi_{i1,j1})].\end{aligned} \tag{12}$$

The second element matrix may then be written

$$\begin{aligned}F_{ij} = l_i l_j [&\phi_{i2,j2} \int_V L_{i1}L_{j1}\, dV - \phi_{i2,j1} \int_V L_{i1}L_{j2}\, dV \\ &- \phi_{i1,j2} \int_V L_{i2}L_{j1}\, dV + \phi_{i1,j1} \int_V L_{i2}L_{j2}\, dV].\end{aligned} \tag{13}$$

This expression may be simplified by employing the general integration formula for 3-D simplex coordinates

$$\iiint_V (L_1)^i (L_2)^j (L_3)^k (L_4)^l\, dV = \frac{3!i!j!k!l!}{(3+i+j+k+l)!} V. \tag{14}$$

In (13), two simplex coordinates (possibly the same) are involved in each integral. These integrals can be expressed in matrix form as

$$M_{ij} = \frac{1}{V} \int_V L_i L_j\, dV = \frac{1}{20} \begin{bmatrix} 2 & 1 & 1 & 1 \\ 1 & 2 & 1 & 1 \\ 1 & 1 & 2 & 1 \\ 1 & 1 & 1 & 2 \end{bmatrix}. \tag{15}$$

Using (15), (13) reduces to

$$\begin{aligned}F_{ij} = V l_i l_j [&\phi_{i2,j2} M_{i1,j1} - \phi_{i2,j1} M_{i1,j2} \\ &- \phi_{i1,j2} M_{i2,j1} + \phi_{i1,j1} M_{i2,j2}].\end{aligned} \tag{16}$$

B. LT/QN Elements

This section presents the linear-tangent, quadratic-normal (LT/QN) element matrices. LT/QN basis functions exist in two forms, edge based and face based functions. The edge based functions can be written in terms of the two simplex coordinates which correspond to the endpoints of an edge, while the face based functions can be written in terms of the three simplex coordinates which correspond to the vertices of a face. The edge based LT/QN basis functions are

$$\left.\begin{aligned}\overline{\boldsymbol{B}}_i^{\mathrm{e1}} &= l_i L_{i1} \nabla L_{i2} \\ \overline{\boldsymbol{B}}_i^{\mathrm{e2}} &= l_i L_{i2} \nabla L_{i1}\end{aligned}\right\} \qquad i = 1, \cdots, 6 \tag{17}$$

where "e1" denotes the first type of edge basis function, and "e2" denotes the second type of edge basis function. The two face-based basis functions associated with face i are

$$\left.\begin{aligned}\overline{\boldsymbol{B}}_i^{\mathrm{f1}} &= L_{i1}L_{i2}\nabla L_{i3} - L_{i1}L_{i3}\nabla L_{i2} \\ \overline{\boldsymbol{B}}_i^{\mathrm{f2}} &= L_{i1}L_{i2}\nabla L_{i3} - L_{i2}L_{i3}\nabla L_{i1}\end{aligned}\right\} \qquad i = 1, \cdots, 4 \tag{18}$$

where "f1" represents the first type of face basis function, and "f2" represents the second. For face-based basis functions, $i1, i2$, and $i3$ indicate the three vertex indices of face i. The element matrices for LT/QN elements involve interactions between the four types of basis functions. Therefore, the element matrices can be represented as block matrices

$$\boldsymbol{E} = \begin{bmatrix} \boldsymbol{E}^{\mathrm{e1e1}} & \boldsymbol{E}^{\mathrm{e1e2}} & \boldsymbol{E}^{\mathrm{e1f1}} & \boldsymbol{E}^{\mathrm{e1f2}} \\ \boldsymbol{E}^{\mathrm{e2e1}} & \boldsymbol{E}^{\mathrm{e2e2}} & \boldsymbol{E}^{\mathrm{e2f1}} & \boldsymbol{E}^{\mathrm{e2f2}} \\ \boldsymbol{E}^{\mathrm{f1e1}} & \boldsymbol{E}^{\mathrm{f1e2}} & \boldsymbol{E}^{\mathrm{f1f1}} & \boldsymbol{E}^{\mathrm{f1f2}} \\ \boldsymbol{E}^{\mathrm{f2e1}} & \boldsymbol{E}^{\mathrm{f2e2}} & \boldsymbol{E}^{\mathrm{f2f1}} & \boldsymbol{E}^{\mathrm{f2f2}} \end{bmatrix} \tag{19}$$

where, for example

$$E_{ij}^{\mathrm{e1f1}} = \int_V \nabla \times \overline{\boldsymbol{B}}_i^{\mathrm{e1}} \cdot \nabla \times \overline{\boldsymbol{B}}_j^{\mathrm{f1}}\, dV. \tag{20}$$

The subscript i in (20) is an edge index and the subscript j is a face index. This is implied by the superscripts, "e1" and "f1", respectively. The second element matrix, F, can be represented similarly

$$\boldsymbol{F} = \begin{bmatrix} \boldsymbol{F}^{\mathrm{e1e1}} & \boldsymbol{F}^{\mathrm{e1e2}} & \boldsymbol{F}^{\mathrm{e1f1}} & \boldsymbol{F}^{\mathrm{e1f2}} \\ \boldsymbol{F}^{\mathrm{e2e1}} & \boldsymbol{F}^{\mathrm{e2e2}} & \boldsymbol{F}^{\mathrm{e2f1}} & \boldsymbol{F}^{\mathrm{e2f2}} \\ \boldsymbol{F}^{\mathrm{f1e1}} & \boldsymbol{F}^{\mathrm{f1e2}} & \boldsymbol{F}^{\mathrm{f1f1}} & \boldsymbol{F}^{\mathrm{f1f2}} \\ \boldsymbol{F}^{\mathrm{f2e1}} & \boldsymbol{F}^{\mathrm{f2e2}} & \boldsymbol{F}^{\mathrm{f2f1}} & \boldsymbol{F}^{\mathrm{f2f2}} \end{bmatrix}. \tag{21}$$

To evaluate each block matrix in (19), the curl of each of the four types of basis functions is needed. For the first type of edge based basis function, "e1", the curl is

$$\nabla \times \overline{\boldsymbol{B}}_i^{\mathrm{e1}} = \nabla \times (l_i L_{i1} \nabla L_{i2}) = l_i \nabla L_{i1} \times \nabla L_{i2} = l_i \overline{v}_{i1,i2}. \tag{22}$$

Similarly, the curl of the second type of edge based basis function, "e2", is

$$\begin{aligned}\nabla \times \overline{\boldsymbol{B}}_i^{\mathrm{e2}} &= \nabla \times (l_i L_{i2} \nabla L_{i1}) = l_i \nabla L_{i2} \times \nabla L_{i1} \\ &= -\nabla \times \overline{\boldsymbol{B}}_i^{\mathrm{e1}} = -l_i \overline{v}_{i1,i2}.\end{aligned} \tag{23}$$

The curl of the first type of face based basis function, "f1", is slightly more complicated.

$$\begin{aligned}\nabla \times \overline{B}_i^{\mathrm{f1}} &= \nabla \times (L_{i1}L_{i2}\nabla L_{i3}) - \nabla \times (L_{i1}L_{i3}\nabla L_{i2}) \\ &= \nabla(L_{i1}L_{i2}) \times \nabla l_{i3} - \nabla(L_{i1}L_{i3}) \times \nabla L_{i2} \\ &= (L_{i1}\nabla L_{i2} + L_{i2}\nabla L_{i1}) \times \nabla L_{i3} \\ &\quad - (L_{i1}\nabla L_{i3} + L_{i3}\nabla L_{i1}) \times \nabla L_{i2} \\ &= 2L_{i1}(\nabla L_{i2} \times \nabla L_{i3}) + L_{i2}(\nabla L_{i1} \times \nabla L_{i3}) \\ &\quad - L_{i3}(\nabla L_{i1} \times \nabla L_{i2}) \\ &= 2L_{i1}\overline{v}_{i2,i3} + L_{i2}\overline{v}_{i1,i3} - L_{i3}\overline{v}_{i1,i2}. \end{aligned} \tag{24}$$

Similarly, the curl of the "f2" function is

$$\nabla \times \overline{B}_i^{\mathrm{f2}} = L_{i1}\overline{v}_{i2,i3} + 2L_{i2}\overline{v}_{i1,i3} + L_{i3}\overline{v}_{i1,i2}. \tag{25}$$

An examination of the original element matrices, (1) and (2), reveals that both are symmetric. Therefore, only those matrices on or above the main diagonal in (19) and (21) need to be evaluated. Using the curl expressions in (22)–(25) and the integration matrix notation of (15), the i, j entries in each of the submatrices in (19) are

$$E_{ij}^{\mathrm{e1e1}} = Vl_il_j(\overline{v}_{i1,i2} \cdot \overline{v}_{j1,j2}) \tag{26}$$

$$E_{ij}^{\mathrm{e1e2}} = Vl_il_j(\overline{v}_{i1,i2} \cdot \overline{v}_{j2,j1}) = -E_{ij}^{\mathrm{e1e1}} \tag{27}$$

$$E_{ij}^{\mathrm{e2e2}} = Vl_il_j(\overline{v}_{i2,i1} \cdot \overline{v}_{j2,j1}) = E_{ij}^{\mathrm{e1e1}} \tag{28}$$

$$E_{ij}^{\mathrm{e1f1}} = \frac{Vl_i}{4}\overline{v}_{i1,i2} \cdot (2\overline{v}_{j2,j3} + \overline{v}_{j1,j3} - \overline{v}_{j1,j2}) \tag{29}$$

$$\begin{aligned}E_{ij}^{\mathrm{e2f1}} &= \frac{Vl_i}{4}\overline{v}_{i2,i1} \cdot (2\overline{v}_{j2,j3} + \overline{v}_{j1,j3} - \overline{v}_{j1,j2}) \\ &= -E_{ij}^{\mathrm{e1f1}} \end{aligned} \tag{30}$$

$$\begin{aligned}E_{ij}^{\mathrm{f1f1}} &= V(4M_{i1,j1}\overline{v}_{i2,i3} \cdot \overline{v}_{j2,j3} + 2M_{i1,j2}\overline{v}_{i2,i3} \\ &\quad \cdot \overline{v}_{j1,j3} - 2M_{i1,j3}\overline{v}_{i2,i3} \cdot \overline{v}_{j1,j2} \\ &\quad + 2M_{i2,j1}\overline{v}_{i1,i3} \cdot \overline{v}_{j2,j3} + M_{i2,j2}\overline{v}_{i1,i3} \\ &\quad \cdot \overline{v}_{j1,j3} - M_{i2,j3}\overline{v}_{i1,i3} \cdot \overline{v}_{j1,j2} \\ &\quad - 2M_{i3,j1}\overline{v}_{i1,i2} \cdot \overline{v}_{j2,j3} - M_{i3,j2}\overline{v}_{i1,i2} \\ &\quad \cdot \overline{v}_{j1,j3} + M_{i3,j3}\overline{v}_{i1,i2} \cdot \overline{v}_{j1,j2}) \end{aligned} \tag{31}$$

$$E_{ij}^{\mathrm{e1f2}} = \frac{Vl_i}{4}\overline{v}_{i1,i2} \cdot (\overline{v}_{j2,j3} + 2\overline{v}_{j1,j3} + \overline{v}_{j1,j2}) \tag{32}$$

$$\begin{aligned}E_{ij}^{\mathrm{e2f2}} &= \frac{Vl_i}{4}\overline{v}_{i2,i1} \cdot (\overline{v}_{j2,j3} + 2\overline{v}_{j1,j3} + \overline{v}_{j1,j2}) \\ &= -E_{ij}^{\mathrm{e1f2}} \end{aligned} \tag{33}$$

$$\begin{aligned}E_{ij}^{\mathrm{f1f2}} &= V(2M_{i1,j1}\overline{v}_{i2,i3} \cdot \overline{v}_{j2,j3} + 4M_{i1,j2}\overline{v}_{i2,i3} \\ &\quad \cdot \overline{v}_{j1,j3} + 2M_{i1,j3}\overline{v}_{i2,i3} \cdot \overline{v}_{j1,j2} \\ &\quad + M_{i2,j1}\overline{v}_{i1,i3} \cdot \overline{v}_{j2,j3} + 2M_{i2,j2}\overline{v}_{i1,i3} \\ &\quad \cdot \overline{v}_{j1,j3} + M_{i2,j3}\overline{v}_{i1,i3} \cdot \overline{v}_{j1,j2} \\ &\quad - M_{i3,j1}\overline{v}_{i1,i2} \cdot \overline{v}_{j2,j3} - 2M_{i3,j2}\overline{v}_{i1,i2} \\ &\quad \cdot \overline{v}_{j1,j3} - M_{i3,j3}\overline{v}_{i1,i2} \cdot \overline{v}_{j1,j2}) \end{aligned} \tag{34}$$

$$\begin{aligned}E_{ij}^{\mathrm{f2f2}} &= V(M_{i1,j1}\overline{v}_{i2,i3} \cdot \overline{v}_{j2,j3} + 2M_{i1,j2}\overline{v}_{i2,i3} \\ &\quad \cdot \overline{v}_{j1,j3} + M_{i1,j3}\overline{v}_{i2,i3} \cdot \overline{v}_{j1,j2} \\ &\quad + 2M_{i2,j1}\overline{v}_{i1,i3} \cdot \overline{v}_{j2,j3} + 4M_{i2,j2}\overline{v}_{i1,i3} \\ &\quad \cdot \overline{v}_{j1,j3} + 2M_{i2,j3}\overline{v}_{i1,i3} \cdot \overline{v}_{j1,j2} \\ &\quad + M_{i3,j1}\overline{v}_{i1,i2} \cdot \overline{v}_{j2,j3} + 2M_{i3,j2}\overline{v}_{i1,i2} \\ &\quad \cdot \overline{v}_{j1,j3} + M_{i3,j3}\overline{v}_{i1,i2} \cdot \overline{v}_{j1,j2}) \end{aligned} \tag{35}$$

The block entries in the second element matrix, (21), follow a similar derivation, to produce

$$F_{ij}^{\mathrm{e1e1}} = Vl_il_j\phi_{i2,j2}M_{i1,j1} \tag{36}$$

$$F_{ij}^{\mathrm{e1e2}} = Vl_il_j\phi_{i2,j1}M_{i1,j2} \tag{37}$$

$$F_{ij}^{\mathrm{e2e2}} = Vl_il_j\phi_{i1,j1}M_{i2,j2} \tag{38}$$

$$F_{ij}^{\mathrm{e1f1}} = Vl_i(\phi_{i2,j3}N_{i1,j1,j2} - \phi_{i2,j2}N_{i1,j1,j3}) \tag{39}$$

$$F_{ij}^{\mathrm{e2f1}} = Vl_i(\phi_{i1,j3}N_{i2,j1,j2} - \phi_{i1,j2}N_{i2,j1,j3}) \tag{40}$$

$$\begin{aligned}F_{ij}^{\mathrm{f1f1}} &= V(\phi_{i3,j3}P_{i1,i2,j1,j2} - \phi_{i3,j2}P_{i1,i2,j1,j3} \\ &\quad - \phi_{i2,j3}P_{i1,i3,j1,j2} + \phi_{i2,j2}P_{i1,i3,j1,j3}) \end{aligned} \tag{41}$$

$$F_{ij}^{\mathrm{e1f2}} = Vl_i(\phi_{i2,j3}N_{i1,j1,j2} - \phi_{i2,j1}N_{i1,j2,j3}) \tag{42}$$

$$F_{ij}^{\mathrm{e2f2}} = Vl_i(\phi_{i1,j3}N_{i2,j1,j2} - \phi_{i1,j1}N_{i2,j2,j3}) \tag{43}$$

$$\begin{aligned}F_{ij}^{\mathrm{f1f2}} &= V(\phi_{i3,j3}P_{i1,i2,j1,j2} - \phi_{i3,j1}P_{i1,i2,j2,j3} \\ &\quad - \phi_{i2,j3}P_{i1,i3,j1,j2} + \phi_{i2,j1}P_{i1,i3,j2,j3}) \end{aligned} \tag{44}$$

$$\begin{aligned}F_{ij}^{\mathrm{f2f2}} &= V(\phi_{i3,j3}P_{i1,i2,j1,j2} - \phi_{i3,j1}P_{i1,i2,j2,j3} \\ &\quad - \phi_{i1,j3}P_{i2,i3,j1,j2} + \phi_{i1,j1}P_{i2,i3,j2,j3}). \end{aligned} \tag{45}$$

The new integration matrices, N and P, are straightforward extensions of M from (15)

$$N_{ijk} = \frac{1}{V}\int_V L_iL_jL_k\, dV \tag{46}$$

and

$$P_{ijkl} = \frac{1}{V}\int_V L_iL_jL_kL_l\, dV. \tag{47}$$

IV. Application to Resonant Cavity Analysis

The element matrices derived above may be used to construct global finite element matrices. This is accomplished by summing the element matrix terms for each tetrahedron in the mesh. With knowledge of the connectivity matrix for the mesh, it is possible to predetermine the sparsity structure of the global matrices. This allows for memory efficient construction of the global matrices in which only nonzero terms are stored. When combined with an iterative eigenvalue solution algorithm, this provides a memory and processor efficient finite element algorithm. The CT/LN and LT/QN basis functions were implemented in the finite element analysis of cavity resonators. To illustrate the relative accuracy of these functions, they were used to estimate the wavenumbers of the vector Helmholtz equation for homogenous media

$$\nabla \times \nabla \times \overline{E} = k^2\overline{E}. \tag{48}$$

The resulting matrix eigensystem was solved for the wavenumbers k, using a sparse solver based on the method of subspace iteration [4].

A rectangular cavity, with dimensions $1 \times 0.5 \times 0.75$ m, was discretized using a commercial software package into six meshes of various density. This package creates unstructured tetrahedral meshes which strive to keep all tetrahedra well-shaped. Table III presents the results for CT/LN basis functions and Table IV presents the results for LT/QN basis functions. The edge lengths in these tables indicate the average length of all the edges in the mesh. Although the convergence

TABLE III
NUMERICAL RESULTS FOR CT/LN BASIS FUNCTIONS

Unknowns	28	75	100	163	227	299	Exact
Edge Length, h	0.44493	0.31161	0.29486	0.25917	0.23571	0.21848	Wavenumber
TE101	4.76396	5.10871	5.17303	5.14063	5.19660	5.19896	5.23599
TE110	6.29049	6.76497	6.90798	6.95349	7.03549	6.90898	7.02481
TE011	7.23955	7.32075	7.23088	7.26992	7.45543	7.42344	7.55145
TE201	7.75215	7.36646	7.63382	7.41055	7.55504	7.46930	7.55145
TM111	7.92726	7.73602	7.98521	7.92726	7.99250	8.02093	8.17887
TE111	8.36779	8.17575	8.29114	8.16214	8.26244	8.13015	8.17887
TM210	8.92183	8.32673	8.36658	8.54727	8.63590	8.69363	8.88577
TE102	9.50991	8.67504	8.88956	8.71941	8.81744	8.92136	8.94726

TABLE IV
NUMERICAL RESULTS FOR LT/QN BASIS FUNCTIONS

Unknowns	204	518	668	1058	1430	1882	Exact
Edge Length, h	0.44493	0.31161	0.29486	0.25917	0.23571	0.21848	Wavenumber
TE101	5.26421	5.23886	5.23524	5.23498	5.23593	5.23671	5.23599
TE110	7.06509	7.03298	7.02931	7.03118	7.02600	7.02800	7.02481
TE011	7.56545	7.56938	7.55086	7.54626	7.55329	7.55216	7.55145
TE201	7.69411	7.57587	7.55620	7.55683	7.55896	7.55491	7.55145
TM111	8.22497	8.20124	8.18831	8.19219	8.18845	8.17913	8.17887
TE111	8.30736	8.21067	8.19727	7.19700	8.19189	8.18344	8.17887
TM210	8.81126	8.92389	8.89925	8.89649	8.89899	8.89752	8.88577
TE102	8.90346	8.97387	8.95721	8.93565	8.95150	8.95565	8.94726

of any particular eigenvalue is usually erratic, the general error behavior of the two methods is apparent when the average error of several modes is visualized. Fig. 2 shows the average percent error of the first eight modes plotted versus the average length, h, of all edges in the mesh. A curve fit through the data points indicates the order of convergence of the two methods. For this geometry, a curve fit to the CT/LN data has an exponent of 1.98, while a similar curve through LT/QN data has exponent 3.86. This $O(h^2)$ convergence for CT/LN elements and $O(h^4)$ convergence for LT/QN elements is consistent with previous 2-D numerical investigations and the theoretical 3-D dispersion analysis of Warren [5]. Similar trends were observed for other cavity geometries including spherical and cylindrical shapes.

As indicated in Fig. 2, on a given mesh, the LT/QN basis functions give much more accurate solutions for the wavenumbers, k, than do CT/LN basis functions. However, for a given mesh, LT/QN basis functions require more unknowns than CT/LN functions. Based on experience, approximately six times as many unknowns are needed for the LT/QN basis functions on a given mesh. Even though LT/QN elements require more unknowns, Fig. 3 demonstrates that for equal numbers of unknowns, LT/QN elements still outperform CT/LN elements.

Higher-order elements also affect the global matrix sparsity characteristics. CT/LN basis functions typically yield global matrices with approximately 15 nonzero entries per row, while LT/QN functions usually give global matrices with approximately 35 nonzero entries per row. This means that LT/QN solutions require more computational effort than

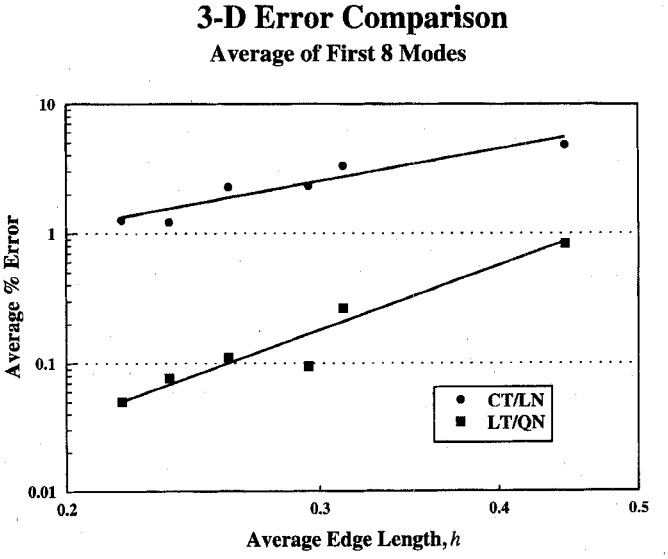

Fig. 2. Error comparison between CT/LN and LT/QN elements based on the average mesh edge length, h. The slope (exponent) of the CT/LN curve fit is 1.98, while the slope of the LT/QN curve fit is 3.86.

CT/LN solutions with an equal number of unknowns. However, in analyses with equal unknowns, CT/LN basis functions require a mesh with many more tetrahedra. This increased mesh density increases the mesh creation time and the mesh storage requirements. Therefore, LT/QN basis functions used with relatively coarse meshes provide more efficient solutions. This assumes that no additional geometry modeling errors are introduced by using a coarse mesh. For arbitrary geometries,

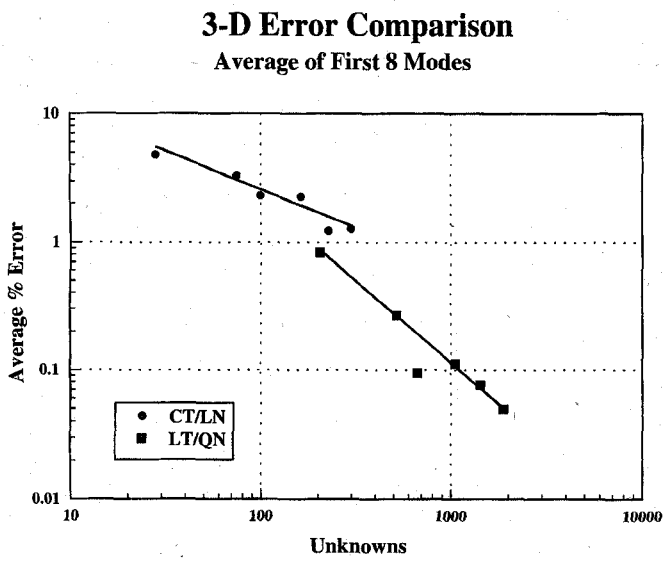

Fig. 3. Error comparison between CT/LN and LT/QN elements based on the number of unknowns. The curves diverge, indicating that LT/QN elements provide more accurate solutions with equivalent computational effort.

this necessitates the use of curved tetrahedra, a subject of future work.

V. Conclusion

This paper has reviewed the first three mixed order, 3-D, vector basis functions for tetrahedra. Element matrices were derived for CT/LN and LT/QN elements. Results were presented from the application of these two basis function sets to cavity resonator analysis. It is concluded that higher order basis functions are preferable to lower order basis functions, since higher order bases are capable of providing more accurate results with coarse tetrahedral meshes, fewer unknowns, and less overall computation. Numerical solutions for the resonant wavenumbers were observed to converge at an $O(h^2)$ rate for the CT/LN functions and an $O(h^4)$ rate for the LT/QN functions.

References

[1] J. C. Nedelec, "Mixed finite elements in R3," *Num. Math.*, vol. 35, pp. 315–341, 1980.
[2] J. F. Lee and R. Mittra, "A note on the application of edge-elements for modeling three-dimensional inhomogeneously-filled cavities," *IEEE Trans. Microwave Theory Tech.*, vol. 40, pp. 1767–1773, Sept. 1992.
[3] J. Jin, "The finite element method in electromagnetics." New York: Wiley, 1993
[4] Y. Li, S. Zhu, and F. A. Fernandez, "The efficient solution of large sparse nonsymmetric and complex eigensystems by subspace iteration," *IEEE Trans. Magn.*, vol. 30, pp. 3582–3585, Sept. 1994.
[5] G. S. Warren, "The analysis of numerical dispersion in the finite-element method using nodal and tangential-vector elements," Ph.D. Dissertation, Georgia Institute of Technology, Atlanta, Georgia, 1995.

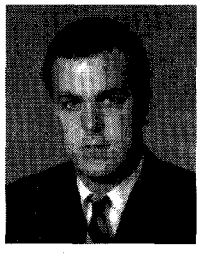

J. Scott Savage (S'95) received the B.E.E. degree from the Georgia Institute of Technology in June, 1992, and the M.S.E.E. degree from the University of Kentucky in December, 1993. Since 1994, he has been a Ph.D. student and Research Assistant at the Georgia Institute of Technology.

From 1992 to 1993, he was a Research Assistant studying crosstalk in cable bundles with Ford Motor Company. His interests include computational and applied electromagnetics.

Mr. Savage is a member of Eta Kappa Nu and Tau Beta Pi.

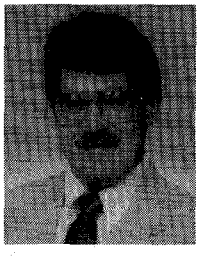

Andrew F. Peterson (S'82–M'83–SM'92) received the B.S., M.S., and Ph.D. degrees in electrical engineering from the University of Illinois, Urbana-Champaign in 1982, 1983, and 1986, respectively.

From 1987 to 1989, he served as Visiting Assistant Professor at the University of Illinois. Since 1989, he has been a member of the faculty of the School of Electrical and Computer Engineering at the Georgia Institute of Technology, where he is now an Associate Professor. He teaches electromagnetic field theory and computational electromagnetics, and conducts research in the development of computational techniques for electromagnetic scattering, microwave devices, and electronic packaging applications. He is an Associate Editor of the IEEE Transactions on Antennas and Propagation.

Dr. Peterson is the immediate past Chairman of the Atlanta chapter of the IEEE AP-S/MTT society. He is also a Director of ACES and a member of URSI Commission B, ASEE, and AAUP.